

Stress Analysis for Thin Bonded Layers

L. M. KEER and Q. GUO

*The Technological Institute, Northwestern University, Evanston,
IL 60208, USA*

ABSTRACT

In this paper the problem of a finite line bond between two thin layers with different elastic and geometric parameters is considered. A system of singular integral equations of the second kind is obtained for the contact stresses along the bonded region. The integral equations can be solved numerically by using an appropriate numerical quadrature scheme. It is found that the evaluation of the kernels is generally difficult for thin layers and a technique using residues is suggested to overcome these difficulties. Numerical results are obtained for some combinations of materials and geometries. It is found that the ratio of the layer thicknesses and shear moduli affects the stress intensity factors when the layer is very thin.

KEYWORDS

Fracture mechanics; bonded elastic layers; composite fracture; debonding of thin layers.

INTRODUCTION

There are many reasons for using coatings and thin films. In the area of microelectronics thin aluminum films are used to carry current in the interior of a chip or an electronic circuit board. In tribology coatings are used to reduce friction or to increase wear resistance. These coating or thin films provide a useful purpose as long as they adhere to the surface. However, one of the common failure modes is delamination and is thus the generic problem of an interfacial crack. Therefore, the analysis for a crack lying along the interface of two elastic bodies is critical.

Williams (1959) first showed through an eigenfunction approach that the near crack-tip field appears to possess an oscillatory singularity. England (1965) and Erdogan (1965) studied the plane problem for a finite length crack at the interface. Erdogan and Aksogan (1974) analyzed the mixed mode behavior of a two-dimensional crack near an interfacial boundary. England (1965) also obtained the explicit forms for the crack opening displacement and showed that this type of oscillation is physically inadmissible because interpenetration near the crack tips will occur. This mathematical difficulty was removed by Comninou (1977) by introducing contact zones. Some techniques to measure adhesion at the interface also have been developed. Charalambides *et al* (1986) proposed a test for determining fracture resistance once the coating

has a crack. Ting *et al* (1985a,b) devised a bending test specimen for the determination of the fracture resistance. Williams (1970) proposed the pressurized blister test to study the strength of the interfacial bonds. A further analysis for the Williams' blister test was made by Farris and Keer (1985).

In this paper, an interfacial external crack problem for two perfectly bonded finite dissimilar infinite strips is discussed. A system of singular integral equations of the second kind was obtained by Keer and Guo (1988) for the normal and shear stresses along the bonded region, and can be solved numerically by using an appropriate quadrature scheme by Miller and Keer (1985) if the kernels can be evaluated properly. For thick layers, the evaluation can be done easily, and some results have been obtained by Keer (1974) and Keer and Guo (1988). However, for thin dissimilar layers the kernels will oscillate, and the evaluation becomes difficult. A technique to evaluate the kernels for thin films is suggested in this paper. Some numerical results are given for both thin and thick layers. It is found that the geometry and material constants have a more important effect on the stress intensity factors for thin layers than for thick layers.

THEORETICAL ANALYSIS

The geometry and coordinate system is as shown in Fig.1. The contact length is $2c$, the shear moduli are μ_1, μ_2 and Poisson's ratios are ν_1, ν_2 . The boundary and continuity conditions can be expressed as

$$\sigma_x(x,y)|_{x=-h_1, h_2} = 0, \quad \sigma_{xy}(x,y)|_{x=-h_1, h_2} = 0 \quad (1.a,b)$$

$$\sigma_x^{(1)}(0,y) = \sigma_x^{(2)}(0,y) = G_1(y)H(c-|y|) \quad (2.a)$$

$$\sigma_{xy}^{(1)}(0,y) = \sigma_{xy}^{(2)}(0,y) = G_2(y)H(c-|y|) \quad (2.b)$$

$$\frac{\partial u^{(1)}(0,y)}{\partial y} = \frac{\partial u^{(2)}(0,y)}{\partial y}, \quad \frac{\partial v^{(1)}(0,y)}{\partial y} = \frac{\partial v^{(2)}(0,y)}{\partial y} \quad (3.a,b)$$

where the superscripts (1) and (2) refer to the upper and the lower layers, respectively, while $H(x)$ is the Heaviside step function.

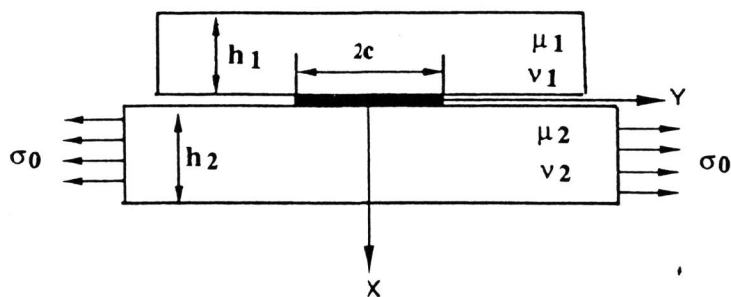


Fig. 1 The geometry and coordinates

A system of singular integral equations of the second kind can be obtained for the stresses $G_1(y)$ and $G_2(y)$ along the bonded region by using the Fourier transform (see Keer (1974) or Keer and Guo (1988) for details). The equations can be written in dimensionless form as

$$\begin{aligned} & \mu_2 \left[\frac{\kappa_1 - 1}{\mu_1} - \frac{\kappa_2 - 1}{\mu_2} \right] f(y) + \frac{\mu_2}{\pi i} \left[\frac{\kappa_1 + 1}{\mu_1} + \frac{\kappa_2 + 1}{\mu_2} \right] \int_{-1}^1 \frac{f(t)}{t-y} dt + \frac{1}{\pi} \int_{-1}^1 K_1(y,t) f(t) dt \\ & + \frac{1}{2\pi i} \int_{-1}^1 K_2(y,t) f(t) dt + \frac{1}{2\pi i} \int_{-1}^1 K_3(y,t) f(t) dt = 1 \end{aligned} \quad (4)$$

with equilibrium condition

$$\int_{-1}^1 f(t) dt = 0 \quad (5)$$

Here, the following dimensionless substitutions are introduced

$$\bar{y} = y/c, \quad \bar{t} = t/c, \quad \bar{h}_1 = h_1/c, \quad \bar{h}_2 = h_2/c, \quad (6)$$

$$f(\bar{y}) = \frac{2}{1+\kappa_2} [G_1(c\bar{y}) + iG_2(c\bar{y})], \quad (7)$$

For the sake of convenience, the $(\bar{\quad})$ notations are dropped in eqn. (4) and thereafter. The kernels $K_1(y,t)$, $K_2(y,t)$ and $K_3(y,t)$ are given in the Appendix.

NUMERICAL ANALYSIS

By using the method given by Miller and Keer (1985), integral equations (4), (5) were solved numerically. Suppose that the solution to eqn. (4) is of the form

$$f(t) = \phi(t)/w(t), \quad w(t) = (1-t)^{\alpha_1} (1+t)^{\alpha_2}, \quad |t| < 1 \quad (8.a,b)$$

where

$$\alpha_1 = \frac{1}{2} + i\beta, \quad \alpha_2 = \frac{1}{2} - i\beta \quad (9.a,b)$$

$$\beta = -\frac{1}{2\pi} \log \left| \frac{\kappa_1 \mu_2 + \mu_1}{\kappa_2 \mu_1 + \mu_2} \right| \quad (9.c)$$

and the function $f(t)$ is approximated by piecewise quadratic functions. The stress intensity factors are defined by

$$K_I + iK_{II} = \sqrt{c} \lim_{y \rightarrow 1} (1-y)^{\alpha_1} (1+y)^{\alpha_2} (\sigma_x + i\sigma_{xy}) = \frac{1+\kappa_2}{2} \sigma_0 \sqrt{c} \phi(1) \quad (10)$$

Because the kernels contain the trigonometric functions of $x(t-y)c/h$ as integrands, which oscillate rapidly when $|t-y|c/h$ is large, the evaluation of the infinite integrals is difficult for large c/h . Thus the numerical results given in most the literature are only for c/h less than about 5. To

find a simple representation for these kernels for large values of $lt-y/c/h$, one can develop a residue expansion by using contour integration in the upper half plane for $K_1(y,t)$ and in the first quadrant for $K_2(y,t)$ and $K_3(y,t)$ in the complex plane.

The poles $z=x+iy$ of the integrands in the complex z plane are determined by the equation

$$e^z + e^{-z} - z^2 - 2 = 0 \quad (11)$$

The location of the k -th pole is found by solving equation (11) numerically. The first several poles in the first quadrant are given in Table 1.

Table 1. Location of poles of the integrands

k	x_k	y_k	k	x_k	y_k
1	4.501457223	8.424784461	6	7.433535359	40.477035416
2	5.537356566	14.995352556	7	7.717617986	46.796710451
3	6.206297492	21.425074794	8	7.966283281	53.109094531
4	6.704419770	27.799919428	9	8.187409850	59.416239651
5	7.102174694	34.146729706	10	8.386502941	65.719482010

By using contour integration in the upper half plane in the complex z plane and eqn. (5), one can obtain

$$\int_{-1}^1 f(t) \int_0^\infty \frac{x^2}{e^x + e^{-x} - x^2 - 2} \cos \frac{x(t-y)}{2h} dx dt = \int_{-1}^1 \left[-3\pi \frac{|t-y|}{h} + \text{Re}(\sum 2\pi i \text{Res} F_1(z_k)) \right] dt \quad (12)$$

where

$$F_1(z) = \frac{1}{2} \frac{z^2}{e^z + e^{-z} - z^2 - 2} \exp(i \frac{z}{2h} |t-y|) \quad (13)$$

and $\text{Res} F_1(z_k)$ stands for the residue of the function F_1 at the k -th pole z_k in the upper half plane. For $K_2(y,t)$, using the contour integration in the first quadrant of the complex z plane, equation (5) and the antisymmetrical property of $G_2(y)$, one can find

$$\int_{-1}^1 f(t) \int_0^\infty \frac{2-2x+x^2-2e^{-x}}{e^x + e^{-x} - x^2 - 2} \left(\sin \frac{x(t-y)}{2h} + \sin \frac{x(t+y)}{2h} \right) dx dt = \int_{-1}^1 f(t) \left[\text{sgn}(t-y) \text{Im}(2\pi i \sum \text{Res} F_2(z_k, |t-y|)) - \text{sgn}(t+y) \text{Im}(2\pi i \sum \text{Res} F_2(z_k, |t+y|)) \right] \frac{2h}{t-y} - \frac{2h}{t+y}$$

$$+ 2\pi \text{sgn}(t-y) + 2\pi \text{sgn}(t+y)] dt \quad (14)$$

where

$$F_2(z, \alpha) = \frac{2-2z+z^2-2e^{-z}}{e^z + e^{-z} - z^2 - 2} \exp(\frac{\alpha z}{2h}) \quad (15)$$

and z_k , which are given in Table 1, represents the k -th pole of F_2 in the first quadrant. Similar residue expansions can be obtained for $K_3(y,t)$.

The evaluation of the kernels consists of the residue expansions, which decay exponentially, provided that $lt-y/h \neq 0$, and hence converge rapidly. The error should be $O(e^{-33lt-y/h})$ for a ten term residue expansion. Thus, this method for the evaluation of the kernels is good for large values of $lt-y/h$. If the interval $[-1,1]$ is divided into N subintervals, the minimum value of $lt-y$ is $1/N$ in Miller and Keer's numerical scheme (1985). The error for $N=10$ and $h \leq 0.25$ should be $O(10^{-6})$. It should be noted that the $1/(t-y)$ term in eqn. (14) appears singular, but is not because the residue expansions are efficient only for large values of $lt-y/h$ and diverge when $t=y$. In our numerical calculations, the residue expansions are used only for $lt-y/h \geq 0.4$.

The numerical results for identical materials and thicknesses for the upper and lower layers are compared with Keer's results (1974), which were obtained by using Erdogan and Gupta's numerical scheme (1972) for this special case. The numerical results obtained from the two different methods are seen to be the same (Table 2).

Table 2. Comparisons of the intensity factors for two identical layers

$\frac{h_1}{c}$	$\frac{K_{II}}{\sigma_0 \sqrt{c}}$ (Keer (1974))	$\frac{K_{II}}{\sigma_0 \sqrt{c}}$ (This analysis)
0.25	.0705	.07054 *
0.5	.0995	.09974 *
1.0	.141	.1410
2.0	.193	.1930

* These two values are obtained by using residue method.

Numerical calculations were carried out for different combinations of materials and geometries. Table 3 gives some numerical results for different shear moduli and Poisson's ratios. Both tables show that the material constants have a more important effect on the stress intensity factors for thin layers than for thick layers, and that the dependence of the stress intensity factors on the Poisson's ratios is significant for a low ratio of the shear modulus of the coating compared to that of the substrate. Table 3.a also shows that the shear moduli do not affect stress intensity factors K_I significantly for thick layers, if the shear modulus of the layer is several times that of the shear modulus of substrate. From table 3.b one can see that the shear moduli have an important effect on the shear intensity factors K_{II} .

Table 4 gives some results for different Poisson's ratios ν_1 and ν_2 , and the thickness ratios h_1/h_2 with $\mu_1 = \mu_2$. From Table 4 one can see that the Poisson's ratio has an important effect on the tensile stress intensity factor, K_I , but not upon the shear stress intensity factors K_{II} . From Table 4 one can also see that, for thick layer problem (i.e. the thickness of the coating is not

Table 3.a The stress intensity factors ($10xK_I\sigma_0\sqrt{c}$) for different shear modulus

h_1/c	μ_1/μ_2 h_2	0.1	0.25	0.5	1.0	2.0	3.0	4.0	6.0	8.0	10.	
		.025	$5h_1$	-.0187	-.0305	-.0269	.0113	.0876	.1644	.2140	.2808	.3227
	∞	-.0195	-.0336	-.0308	.0240	.1934	.3695	.5323	.8141	1.045	1.239	$\nu_2=0.3$
	$5h_1$	-.0128	-.0161	-.0013	.0495	.1425	.2083	.2552	.3158	.3524	.3760	$\nu_1=0.3$
	∞	-.0134	-.0175	.0013	.0828	.2871	.4839	.6602	.9566	1.195	1.390	$\nu_2=0.3$
	$5h_1$	-.0025	.0069	.0361	.1002	.1973	.2596	.3019	.3542	.3842	.4025	$\nu_1=0.4$
	∞	-.0024	.0091	.0508	.1665	.4115	.6307	.8205	1.130	1.373	1.568	$\nu_2=0.3$
1.	$5h_1$.0746	.1836	.3395	.5583	.7818	.8804	.9281	.9643	.9715	.9696	$\nu_1=0.2$
	∞	.0752	.1864	.3479	.5791	.8230	.9356	.9933	1.042	1.058	1.061	$\nu_2=0.3$
	$5h_1$.1071	.2483	.4325	.6668	.8781	.9582	.9908	1.007	1.002	.9922	$\nu_1=0.3$
	∞	.1079	.2520	.4432	.6919	.9252	1.020	1.062	1.090	1.092	1.088	$\nu_2=0.3$
	$5h_1$.1539	.3388	.5578	.8048	.9920	1.046	1.059	1.051	1.033	1.015	$\nu_1=0.4$
	∞	.1550	.3439	.5717	.8358	1.047	1.115	1.138	1.140	1.128	1.115	$\nu_2=0.3$

Table 3.b The stress intensity factors ($10xK_{II}\sigma_0\sqrt{c}$) for different shear modulus

h_1/c	μ_1/μ_2 h_2	0.1	0.25	0.5	1.0	2.0	3.0	4.0	6.0	8.0	10.	
		.025	$5h_1$.0386	.0924	.1678	.2745	.3940	.4597	.5022	.5572	.5932
	∞	.0406	.1039	.2071	.3911	.6797	.9004	1.079	1.362	1.581	1.761	$\nu_2=0.3$
	$5h_1$.0461	.1066	.1866	.2939	.4092	.4721	.5134	.5674	.6033	.6307	$\nu_1=0.3$
	∞	.0488	.1215	.2355	.4321	.7337	.9630	1.148	1.441	1.668	1.851	$\nu_2=0.3$
	$5h_1$.0545	.1215	.2052	.3113	.4223	.4832	.5239	.5780	.6150	.6431	$\nu_1=0.4$
	∞	.0581	.1410	.2661	.4754	.7921	1.032	1.227	1.532	1.767	1.956	$\nu_2=0.3$
1.	$5h_1$.3372	.7210	1.175	1.754	2.416	2.821	3.105	3.489	3.739	3.915	$\nu_1=0.2$
	∞	.3385	.7273	1.192	1.791	2.485	2.913	3.215	3.624	3.892	4.082	$\nu_2=0.3$
	$5h_1$.3539	.7555	1.230	1.835	2.523	2.938	3.226	3.605	3.847	4.015	$\nu_1=0.3$
	∞	.3554	.7524	1.248	1.875	2.597	3.037	3.343	3.748	4.007	4.188	$\nu_2=0.3$
	$5h_1$.3731	.7959	1.296	1.934	2.654	3.079	3.367	3.737	3.967	4.124	$\nu_1=0.4$
	∞	.3748	.8035	1.316	1.978	2.735	3.185	3.492	3.889	4.136	4.305	$\nu_2=0.3$

very much smaller than the contact length), the solution for a half-plane substrate provides a good approximation, if the thickness of the substrate is several times that of the thickness of coating, but this conclusion is not true for the thin layer problem.

Table 4 The effect of Poisson's ratio on the stress intensity factors ($10xK\sigma_0\sqrt{c}$)

h_2/h_1	h_1 ν_1 ν_2	0.025 c			c			
		0.4	0.3	0.2	0.4	0.3	0.2	
5	0.4	K_I	.04951	.00592	-.02592	.66681	.54241	.44601
		K_{II}	.29385	.27113	.24849	1.8348	1.7421	1.6662
	0.3	K_I	.10024	.04951	.01133	.80483	.66681	.55831
		K_{II}	.31129	.29387	.27446	1.9337	1.8348	1.7542
	0.2	K_I	.14955	.09301	.04951	.93662	.78553	.66681
		K_{II}	.32064	.30918	.29388	2.0251	1.9201	1.8348
10	0.4	K_I	.06572	.01154	-.02688	.68691	.55869	.45804
		K_{II}	.35622	.32408	.29332	1.8649	1.7696	1.6916
	0.3	K_I	.13062	.06571	.01819	.82943	.68691	.57507
		K_{II}	.38267	.35608	.32864	1.9665	1.8649	1.7820
	0.2	K_I	.19523	.12122	.06572	.96572	.80948	.68691
		K_{II}	.39856	.37911	.35613	2.0604	1.9525	1.8649
∞	0.4	K_I	.08285	.01605	-.02955	.69193	.56263	.46119
		K_{II}	.43226	.38453	.34201	1.8750	1.7787	1.6998
	0.3	K_I	.16650	.08283	.02405	.83575	.69193	.57913
		K_{II}	.47538	.43213	.39111	1.9778	1.8750	1.7912
	0.2	K_I	.25370	.15420	.08283	.97339	.81561	.69193
		K_{II}	.50655	.46971	.43216	2.0728	1.9636	1.8750

CONCLUSION

An interfacial external crack between two perfectly bonded finite dissimilar infinite strips is discussed, and a numerical technique applicable for a thin layer is suggested. Some results are given for both thick and thin layers. It is found that the stress intensity factors for thin layers (but not necessarily thick layers) are sensitive to the ratio of the thicknesses and the elastic constants. Furthermore, the geometries and the material constants on the stress intensity factors is more significant for the thin layers than for thick layers. The Poisson's ratios have an important effect on stress intensity factors for low ratios of the shear modulus of the coating to that of the substrate. The stress intensity factors K_I and K_{II} are not too dependent on ratio of the shear moduli when the magnitude of the shear modulus of the layer is much greater than that of the substrate; however, for thin layers the opposite is the case.

ACKNOWLEDGMENTS

The authors are grateful to Mr. Mark Hanson for many helpful discussions. Partial support of this research is acknowledged from the Center for Engineering Tribology.

REFERENCES

Charalambides, P.G., J. Lund, A.G. Evans and R.M. McMeeking (1988). "A test specimen for determining the fracture resistance of bimaterial interfaces", Private Communication (to be published).

Comninou, M. (1977). The interfacial crack. *J. appl. Mech.*, 44, 631-636.

England, A.H. (1965). A crack between dissimilar media. *J. appl. Mech.*, 32, 400-402.

Erdogan, F. (1965). Stress distribution in bonded dissimilar materials with cracks. *J. appl. Mech.*, 32, 403-410.

Erdogan, F. and O. Aksogan (1974). Bonded half-planes containing an arbitrarily oriented crack. *Int. J. Solid Structures*, 10, 569-585.

Erdogan, F. and G.D. Gupta (1972). *Quart. Appl. Math.*, 29, 523.

Farris, T.N. and L.M. Keer (1985), Williams' blister test analyzed as an interface crack. *Int. J. Fracture*, 27, 91-103.

Keer, L.M. (1974). Stress analysis for bonded layers. *J. appl. Mech.*, 41, 679-683.

Keer, L.M. and Q. Guo (1988). Stress analysis for symmetrically loaded bonded layers. *Int. J. Fracture*. (in press).

Miller, G.R. and L.M. Keer (1985). A numerical technique for the solution of singular integral equations of the second kind. *Quart. Appl. Math.*, 42, 455-465.

Ting, B.Y., S. Ramalingam and W.O. Winer (1985). An experimental investigation of the film-to-substrate bond strength of sputtered thin film using a semi-quantitative test method. *J. Tribology*, 107, 478-482.

Ting, B.Y., W.O. Winer and S. Ramalingam (1985). A semi-quantitative method for thin film adhesion measurement. *J. Tribology*, 107, 472-477.

Williams, M.L. (1959) The stresses around a fault or crack in dissimilar media. *Bull. Seismol. Soc. Amer.*, 49, 199-204.

Williams, M.L. (1970). The fracture threshold for an adhesive interlayer. *J. Appl. Polym. Sci.*, 14, 1121.

APPENDIX

$$k_2(y,t) = (1+\kappa_1) \frac{\mu_2}{\mu_1} \frac{1}{2h_1} \int_0^\infty \frac{2-2x+x^2-2e^{-x}}{e^x+e^{-x}-x^2-2} \sin \frac{x(t-y)}{2h_1} dx +$$

$$(1+\kappa_2) \frac{1}{2h_2} \int_0^\infty \frac{2-2x+x^2-2e^{-x}}{e^x+e^{-x}-x^2-2} \sin \frac{x(t-y)}{2h_2} dx \tag{A1}$$

$$k_3(y,t) = (1+\kappa_1) \frac{\mu_2}{\mu_1} \frac{1}{2h_1} \int_0^\infty \frac{2+2x+x^2-2e^{-x}}{e^x+e^{-x}-x^2-2} \sin \frac{x(t-y)}{2h_1} dx +$$

$$(1+\kappa_2) \frac{1}{2h_2} \int_0^\infty \frac{2+2x+x^2-2e^{-x}}{e^x+e^{-x}-x^2-2} \sin \frac{x(t-y)}{2h_2} dx \tag{A2}$$

$$K_1(y,t) = (1+\kappa_1) \frac{\mu_2}{\mu_1} \frac{1}{2h_1} \int_0^\infty \frac{x^2}{e^x+e^{-x}-x^2-2} \cos \frac{x(t-y)}{2h_1} dx -$$

$$(1+\kappa_2) \frac{1}{2h_2} \int_0^\infty \frac{x^2}{e^x+e^{-x}-x^2-2} \cos \frac{x(t-y)}{2h_2} dx \tag{A3}$$

$$K_2(y,t) = k_2(y,t) - k_2(y,-t), \quad K_3(y,t) = k_3(y,t) + k_3(y,-t). \tag{A4}$$